

Intermodal energy transfers in a proper orthogonal decomposition–Galerkin representation of a turbulent separated flow

By M. COUPLET¹, P. SAGAUT^{2,1} AND C. BASDEVANT^{3,1}

¹ONERA, DSNA, 29 av. de la Division Leclerc, 92322 Châtillon, France

²Laboratoire de Modélisation en Mécanique, Université Pierre et Marie Curie, Boite 162,
4 place Jussieu, 75252 Paris Cedex 5, France

³Laboratoire de Météorologie Dynamique, École Normale Supérieure, 24 rue Lhomond,
75231 Paris Cedex 5, France

(Received 28 January 2003 and in revised form 18 June 2003)

Energy transfers between modes obtained from the proper orthogonal decomposition (POD) of a turbulent flow past a backward-facing step are analysed with the aim of providing guidelines for modelling unresolved modes in truncated POD–Galerkin models. It is observed that energy transfers are local in the POD basis, and that the Fourier-decomposition-based concepts of forward and backward energy cascades are also valid in the POD basis, the net effect being a forward energy cascade. General features of the eddy-viscosity representation of kinetic energy transfers are investigated through *a priori* tests. It is observed that the ideal eddy-viscosity model should exhibit a cusp behaviour near the cutoff mode.

1. Introduction

The proper orthogonal decomposition (POD, also known as the Karhunen–Loève decomposition, see Holmes, Lumley & Berkooz 1996 for a survey) is a convenient tool for describing non-homogeneous turbulent flows. Indeed, it makes it possible to educe global coherent structures of the flow in an unequivocal way. This decomposition being optimal, it became a popular way to construct dynamical systems representing turbulent flows.

The present paper aims to describe the global features of energy transfers between POD modes in a turbulent, wall-bounded, non-homogeneous separated flow. In particular, a quantitative analysis of the modal interactions, based on computations of eddy-viscosity-like parameters, is proposed. The selected configuration is the turbulent flow past a backward-facing step, with a turbulent inlet. The purpose is twofold.

First, energy transfers have historically been studied using Fourier decomposition, which is convenient for homogeneous flows only; thus, both theoretical (e.g. Kraichnan 1971) and numerical studies (e.g. Yeung, Brasseur & Wang 1995) have provided deep insight into the dynamics of turbulent fluctuations, assessing the existence of forward and backward energy cascades. A few studies based on the POD approach have addressed non-homogeneous turbulent flows, but generally in local configurations such as the minimal channel unit (Aubry *et al.* 1988; Podvin & Lumley 1998; Podvin 2001; Webber, Handler & Sirovich 1997, 2002), or a transient flat-plate boundary layer (Rempfer & Fasel 1994). Here, the POD–Galerkin method is applied to a

spatially extended, non-homogeneous separated flow. Moreover, as POD is equivalent to the Fourier decomposition in homogeneous directions, most authors apply an explicit hybrid POD/Fourier decomposition (Fourier decomposition in homogeneous directions followed by POD in the remaining directions). Such an approach is different from the full three-dimensional POD adopted in this study as far as mode selection is concerned, since the way the modes will be ordered are different: in the full POD, all modes are uniquely ordered (by their eigenvalues), while they can be ordered separately in each homogeneous direction in hybrid Fourier/POD analysis. As previously proposed in Rempfer & Fasel (1994), one goal here is to analyse the energy transfers within a full POD basis, looking at their main characteristics and comparing them with results drawn from the Fourier analysis in the isotropic case.

Secondly, when turbulent flows are considered, although very few POD modes contain most of the total turbulent kinetic energy and can be kept to construct a reduced-order dynamical system, the low-energetic modes, which drop out, must be taken into account in the POD–Galerkin approach to recover an accurate description of the flow. This problem is formally equivalent to that of large-eddy simulation (LES, see Sagaut 2002 for a general presentation). Following the proposal of Aubry *et al.* (1988), most authors use a diffusive model based on an extension of the Heisenberg spectral viscosity model for homogeneous flows: Berkooz *et al.* (1990); Podvin (2001); Ukeiley *et al.* (2001). As quoted by Aubry *et al.* (1988), such a model is very similar to the well-known Smagorinsky one, which can be interpreted as an extension of the same Heisenberg model in physical space for flows represented using a local basis. However, as previously mentioned, almost all works using that approach rely on a POD/Fourier decomposition (e.g. two-homogeneous-direction plane channel flow). Truncating the basis in both the Fourier and POD representation, the validity of the parameterization of unresolved modes using a viscosity-type model may be understood by invoking the Kolmogorov hypothesis and assuming that the cutoff occurs at small enough scales, as is done in the usual LES framework. The validity of this model for the minimal channel flow unit was assessed by Podvin (2001). However, when considering complex non-homogeneous flows, the question may arise of the validity of this type of eddy-viscosity model, since the underlying assumptions dealing with both the existence and the dominance of a forward energy cascade remain to be investigated. The second goal of the present study is therefore to provide an analysis of the representation of the energy transfers between modes via an eddy-viscosity assumption, in order to provide guidelines for the definition of models for the unresolved modes. Since it is known that even in the simple case of the Fourier representation of isotropic turbulence the global features of subgrid models are very dependent on the spectrum shape, the filter shape and the cutoff length, the case of truncated POD models is non-trivial.

2. Numerical database and POD–Galerkin method

The POD modes are computed using $M = 1000$ three-dimensional instantaneous snapshots obtained by performing a LES of a turbulent incompressible flow past a backward-facing step. The Reynolds number based on the mean streamwise velocity at the entrance and the height of the channel above the step is 66 100. That based on the inflow velocity Γ_{in} and the height h of the step is 7432. The three velocity components are stored over the full computational domain every 50 time steps. The computational domain (see figure 1) contains the turbulent inlet channel and the flow past the step. The sampling time is chosen so as to encompass at least one period of

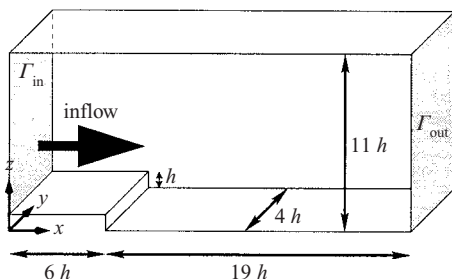


FIGURE 1. Geometry of the computational domain, corresponding to the spatial extent of the POD modes.

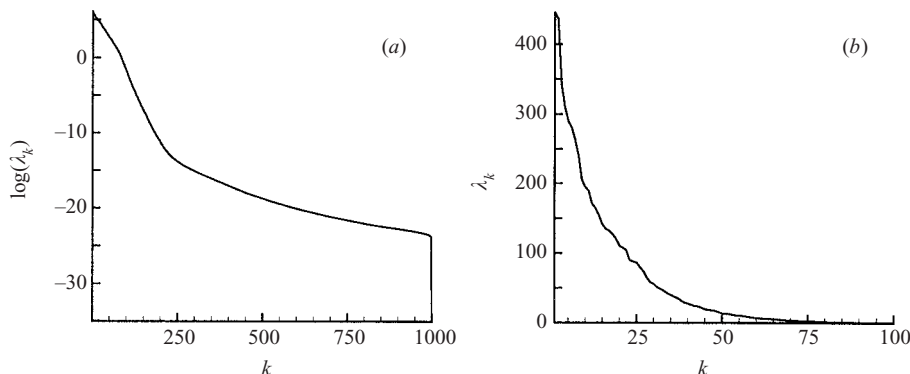


FIGURE 2. (a) Full POD spectrum; (b) first 100 POD modes.

the low-frequency breathing mode of the recirculation bubble. The reader is referred to Labbé, Sagaut & Montreuil (2002) for details on the LES.

The instantaneous velocity field \mathbf{u} is split into a mean part $\bar{\mathbf{u}}(x, y, z) = \langle \mathbf{u}(x, y, z, t) \rangle$ and a fluctuating part $\tilde{\mathbf{u}} = \mathbf{u} - \bar{\mathbf{u}}$, where $\langle \cdot \rangle$ denotes the average over the M snapshots. The POD decomposition is applied to $\tilde{\mathbf{u}}$, yielding

$$\tilde{\mathbf{u}}(x, y, z, t) = \sum_k \underbrace{(\tilde{\mathbf{u}}, \boldsymbol{\phi}_k)}_{\tilde{a}_k(t)} \boldsymbol{\phi}_k(x, y, z) \tag{2.1}$$

where (\cdot, \cdot) is the classical L^2 inner product on the flow domain. $(\boldsymbol{\phi}_k)_{k \in \llbracket 1, M \rrbracket}$ is the orthonormal POD basis and the $\tilde{a}_k(t)$ the time-dependent coefficients of the decomposition. They have the following orthogonality property:

$$\langle \tilde{a}_k \tilde{a}_j \rangle = \lambda_k \delta_{j,k} = \sigma_k^2 \delta_{j,k} \quad \forall k, j \tag{2.2}$$

and the basis is ordered so that $\lambda_k \geq \lambda_{k+1} \forall k$.

This decomposition is optimal in the sense that, for all n , the first n POD modes capture more kinetic energy on the average than any other set of n spatial functions. Figure 2 displays the POD spectrum on a logarithmic scale computed from the database. One of the main advantage of the POD basis, thanks to its optimality property, is that it allows very large data compression factors. In the present case, the first 87 modes contain 99.9% of the mean turbulent kinetic energy.

To analyse energy transfers among POD modes, the evolution equation for each mode is obtained by applying the Galerkin method on the space spanned by the

first $n \leq M$ POD modes. Considering periodic boundary conditions in the spanwise direction y , the no-slip condition at solid walls, a Dirichlet condition on velocity at the inflow plane, Γ_{in} , where values were prescribed using a precursor simulation of a turbulent incompressible plane channel flow, and the zero-stress outflow boundary condition on the exit plane, the following weak formulation is obtained from the non-dimensional-Navier–Stokes set of equations:

$$\left(\frac{\partial \mathbf{u}}{\partial t} + (\mathbf{u} \cdot \nabla) \mathbf{u}, \boldsymbol{\phi} \right) + \frac{1}{Re} \left[\sum_{v \in \{x,y,z\}} (\nabla u_v, \nabla \phi_v) \right] + \underbrace{\int_{\Gamma_{in}} \left(p n - \frac{1}{Re} \nabla \mathbf{u} \cdot \mathbf{n} \right) \cdot \boldsymbol{\phi} \, d\sigma}_{\text{inlet boundary term}} = 0 \tag{2.3}$$

for all solenoidal test functions $\boldsymbol{\phi}$ satisfying periodic boundary conditions in spanwise direction and the no-slip condition at solid walls. The POD–Galerkin system is obtained by taking the first n modes as basis and test functions. Making the assumption that the inlet boundary term can be neglected (this is realistic since modes arising from the decomposition of $\tilde{\mathbf{u}}$ have very small contributions on the inlet plane Γ_{in}), the following n -dimensional polynomial dynamical system is derived:

$$\dot{a}_i(t) = p_i(A(t)) \quad \forall i \in \llbracket 1, n \rrbracket \tag{2.4}$$

where $A(t) = (a_1(t), \dots, a_n(t))$ and $a_k = \tilde{a}_k / \sigma_k$ for all k . Each p_i can be expressed as

$$p_i(A) = C_i^0 + \frac{D_i^0}{Re} + \sum_{k=1}^n \left(C_i^k + \frac{D_i^k}{Re} \right) a_k + \sum_{k_1=1}^n \sum_{k_2=1}^{k_1} C_i^{k_1, k_2} a_{k_1} a_{k_2} \tag{2.5}$$

with

$$C_i^0 = -((\bar{\mathbf{u}} \cdot \nabla) \bar{\mathbf{u}}, \boldsymbol{\phi}_i), \quad D_i^0 = - \sum_{v \in \{x,y,z\}} (\nabla \bar{u}_v, \nabla (\boldsymbol{\phi}_i)_v), \tag{2.6}$$

$$C_i^k = -\sigma_k ((\boldsymbol{\phi}_k \cdot \nabla) \bar{\mathbf{u}} + (\bar{\mathbf{u}} \cdot \nabla) \boldsymbol{\phi}_k, \boldsymbol{\phi}_i), \quad D_i^k = -\sigma_k \sum_{v \in \{x,y,z\}} (\nabla (\boldsymbol{\phi}_k)_v, \nabla (\boldsymbol{\phi}_i)_v), \tag{2.7}$$

and

$$C_i^{k_1, k_2} = -\frac{\sigma_{k_1} \sigma_{k_2}}{1 + \delta_{k_1, k_2}} [((\boldsymbol{\phi}_{k_1} \cdot \nabla) \boldsymbol{\phi}_{k_2}, \boldsymbol{\phi}_i) + ((\boldsymbol{\phi}_{k_2} \cdot \nabla) \boldsymbol{\phi}_{k_1}, \boldsymbol{\phi}_i)]. \tag{2.8}$$

3. Intermodal kinetic energy transfers

The total fluctuating kinetic energy per mass unit is $K(t) = \frac{1}{2} \|\tilde{\mathbf{u}}\|^2 = \sum_i K_i(t)$ where $K_i(t) = \frac{1}{2} \lambda_i a_i(t)^2$ is the energy captured by the i th mode. From (2.5), we obtain

$$\dot{K}_i = \lambda_i a_i \dot{a}_i = \underbrace{\tilde{C}_i^0 a_i}_{\text{diadic interactions}} + \underbrace{\sum_{k=1}^n \tilde{C}_i^k a_k a_i + \sum_{k_1=1}^n \sum_{k_2=1}^{k_1} \tilde{C}_i^{k_1, k_2} a_{k_1} a_{k_2} a_i}_{\text{triadic interactions}} \tag{3.1}$$

where

$$\tilde{C}_i^0 = \lambda_i \left(C_i^0 + \frac{D_i^0}{Re} \right), \quad \tilde{C}_i^k = \lambda_i \left(C_i^k + \frac{D_i^k}{Re} \right), \quad \tilde{C}_i^{k_1, k_2} = \lambda_i C_i^{k_1, k_2}. \tag{3.2}$$

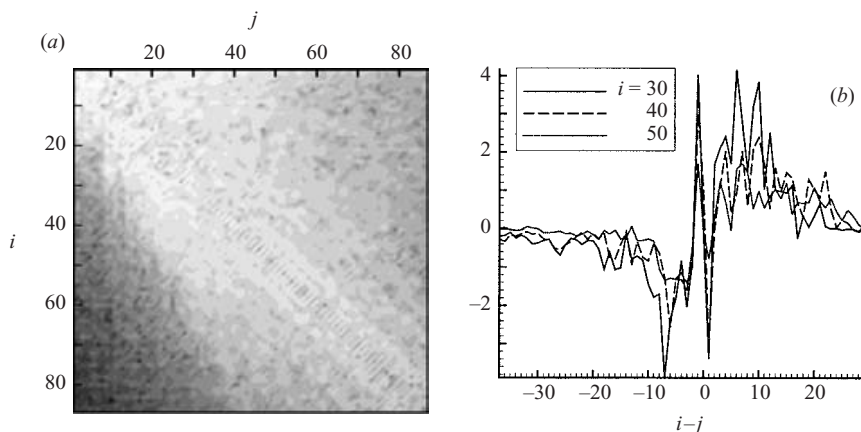


FIGURE 3. (a) Map of $\log(|\langle \Pi(i|j) \rangle|)$: iso-levels, ranging from white (maximum) to black (minimum). (b) $\langle \Pi(i|j) \rangle$ as a function of $(i - j)$ for three values of i .

Equation (3.1) shows that the evolution of the energy of a mode results from three kinds of interactions: a linear interaction with the mean flow, diadic terms arising from the interaction with the mean flow and viscous terms, and triadic interactions which account for the nonlinear inviscid interactions between modes. With the Fourier basis, diadic terms degenerate into simple linear terms, while triadic interactions are non-zero only for specific triads. Therefore differences between POD and usual Fourier decomposition are that viscous terms yield interactions between modes and that all groups of three modes lead to energy transfers. However it is worth noting that mean energy exchanges between POD modes through diadic interactions are zero since $\langle a_i a_j \rangle = \delta_{i,j}$.

Energetic exchanges via triadic interactions are now considered. The triadic term $\tilde{C}_i^{k_1, k_2} a_{k_1} a_{k_2} a_i$ is regarded as the influence of the mode whose index is $\max(k_1, k_2)$ on the variation of K_i . Thus, the influence of the j th mode on the energy of the i th mode is

$$\Pi(i|j) = \sum_{k=1}^j \tilde{C}_i^{j,k} a_k a_j a_i. \quad (3.3)$$

The absolute value of the mean transfer $\langle \Pi(i|j) \rangle$ for the first 87 modes is presented in figure 3; both the global energy transfer map, using a logarithmic scale for a clarity, and profiles for three values of i are plotted. It is observed that energy transfers among POD modes are local; indeed, the mean transfer is negligible for modes (i, j) such that $|i - j| \geq 25$. That property of locality was raised by the results of Rempfer & Fasel (1994), but for a transitional flow and in a small three-dimensional window of the whole initial computational domain. It can be seen as an extension of the well-known result that a Fourier mode with wavenumber k will exchange most of its energy with modes within the range $[k/2, 2k]$, i.e. that energy transfers are local, Kraichnan (1971, 1976). This observation is consistent with the result that POD modes converge toward Fourier modes in the limit of very high wavenumber, i.e. for dissipative scales (see Foias, Manley & Sirovich 1990), but it was not *a priori* obvious in the present case since the cutoff occurs within larger scales. Moreover, analyses carried out on the Fourier basis deal only with homogeneous turbulence and with the inertial range of the spectrum, whereas in the present case, the flow is non-homogeneous, wall

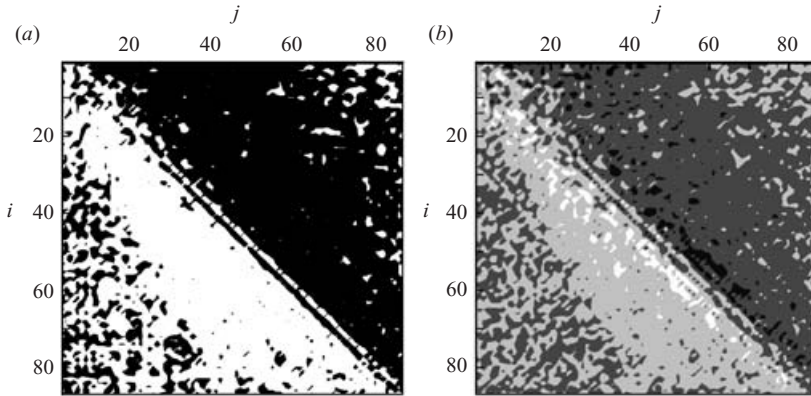


FIGURE 4. (a) Sign of the mean triadic transfer term $\langle \Pi(i|j) \rangle$. Black: negative; white: positive. (b) Percentage of time during which $\Pi(i|j)$ is positive (minimum: 27.5%; maximum: 77.7%) with four grey levels ranging from black to white: [27.5, 40], [40, 50], [50, 60] and [60, 77.7].

bounded and separated, and POD modes are global, i.e. they integrate the dynamics over the whole computational domain.

The direction of transfer is recovered by looking at the sign of the mean transfer term $\langle \Pi(i|j) \rangle$. The corresponding map is displayed in figure 4. Black regions correspond to a negative mean value, i.e. to a net drain of the kinetic energy of mode i by mode j , and white regions to a positive sign, i.e. to a net gain of kinetic energy by mode i . In good agreement with results from Fourier decomposition, it is observed that the main phenomenon is a forward energy cascade among the POD modes: a mode i drains energy from modes $j < i$ and redistributes energy toward modes $k > i$. Some small regions corresponding to an inverse cascade are also detected, but they are associated with very small absolute values of the mean transfer, and thus should not be considered as evidence for the existence of an inverse cascade in the mean.

To obtain a deeper insight into the dynamics of POD modes, the percentage of time during which the instantaneous transfer term $\Pi(i|j)$ is positive is plotted in figure 4. It is seen that net energy gains (resp. losses) are associated with regions where the transfer is most of the time in the same direction as the mean transfer, but that the transfer between two modes is in both directions during the full integration time. This can be interpreted as a generalization of the classical finding of the existence of a backward energy transfer among Fourier modes, or the fact that the sign of local transfers across a cutoff wavenumber may change from time to time and point to point in physical space.

It was observed that the fluctuating kinetic energy transfer among POD modes exhibits many features already observed using a Fourier-mode decomposition. This similarity can be explained by looking at the flow structures associated with each POD mode. Some of them are shown in figure 5, where isosurfaces of the Q-criterion (Hunt, Wray & Moin 1988) are displayed. It is seen that the higher the index of the POD mode is, the smaller are the flow structures. This is consistent with the fact that POD modes are sorted by decreasing order of kinetic energy, and that small structures are less energetic than larger ones. So, in agreement with Kolmogorov's local isotropy hypothesis, the main conclusions from the Fourier analysis can be extended to the POD decomposition framework. Consequently, the main phenomenon is a cascade

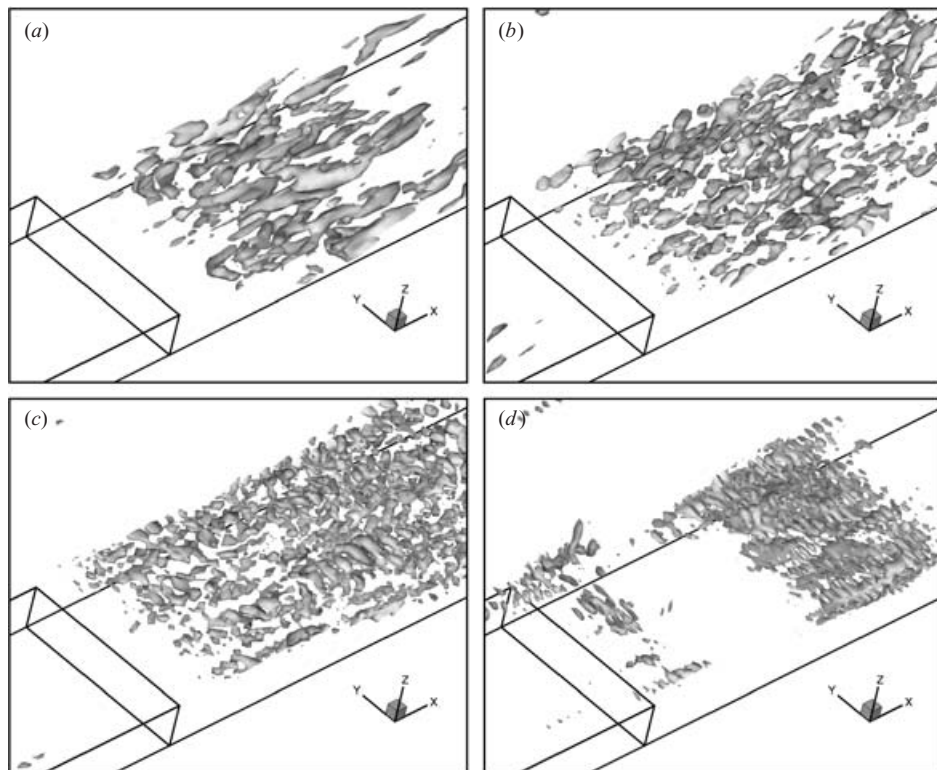


FIGURE 5. Isosurfaces of the Q criterion for some POD modes: (a) ϕ_1 with $Q = Q_1$; (b) ϕ_{20} with $Q = \frac{2}{3}Q_1$; (c) ϕ_{42} with $Q = \frac{10}{3}Q_1$; (d) ϕ_{87} with $Q = \frac{10}{3}Q_1$.

of kinetic energy from low- toward high-index modes. This forward cascade is a net effect, and some inverse cascade transfers occur over short durations, yielding an inverse cascade.

4. On eddy-viscosity parameterization of kinetic energy transfers

We now analyse the POD modal interactions through the computations of pseudo-eddy-viscosities, with emphasis on the parameterization of the energy transfers across a cutoff index l . This, which is an extension of the usual LES closure problem, is encountered when a truncated POD basis is used, i.e. when some POD modes are discarded. Since the use of POD leads to optimal data compression, very-low-order models can be obtained from the POD–Galerkin method, which will mimic either DNS or LES. In the case of LES-like dynamical systems, the problem of taking into account interactions with discarded modes should be solved. The global features of eddy-viscosity type models for POD need to be determined, since many studies carried out in the Fourier framework (e.g. Domaradzki *et al.* 1993, Zhou & Vahala 1993) have shown that the eddy-viscosity representation is very dependent on many parameters (e.g. spectrum shape, filter shape, cutoff wavenumber). A similar analysis is provided here which is expected to give useful informations to improve an LES-like POD–Galerkin model.

Introducing the cutoff index l in (2.5), the resolved (denoted by the \leq exponent) and unresolved interactions ($>$ exponent) terms are

$$p_i(A) = c_i^{\leq}(A) + c_i^{>}(A) + (d_i^{\leq}(A) + d_i^{>}(A))/Re \tag{4.1}$$

with

$$c_i^{\leq}(A) = C_i^0 + \sum_{k=1}^l C_i^k a_k + \sum_{k_1=1}^l \sum_{k_2=1}^{k_1} C_i^{k_1, k_2} a_{k_1} a_{k_2}, \quad d_i^{\leq}(A) = D_i^0 + \sum_{k=1}^l D_i^k a_k, \tag{4.2}$$

$$c_i^{>}(A) = \sum_{k=l+1}^n C_i^k a_k + \sum_{k_1=l+1}^n \sum_{k_2=1}^{k_1} C_i^{k_1, k_2} a_{k_1} a_{k_2} \quad \text{and} \quad d_i^{>}(A) = \sum_{k=l+1}^n D_i^k a_k. \tag{4.3}$$

Corresponding terms arising from (3.1) are $a_i c_i^{\leq}(A)$, $a_i d_i^{\leq}(A)$, $a_i c_i^{>}(A)$ and $a_i d_i^{>}(A)$. The closure problem consists in expressing unresolved terms in the momentum equation and/or the kinetic energy equation as functions of the resolved modes. We consider here eddy-viscosity-type closures, which can be expressed as

$$p_i(A) \approx c_i^{\leq}(A) + (1/Re + \nu(i|l))d_i^{\leq}(A), \quad \text{i.e.} \quad p_i^{\approx} \approx \nu(i|l)d_i^{\leq} \tag{4.4}$$

with $p_i^{\approx} = c_i^{>} + d_i^{>}/Re$. The pseudo eddy-viscosity $\nu(i|l)$ *a priori* depends on the index of the mode considered and on the cutoff index, as is the case for the Kraichnan–Chollet–Lesieur subgrid viscosity in Fourier space (see Kraichnan 1976; Chollet & Lesieur 1981). Two ways computing values of this closure parameter $\nu(i|l)$ are investigated below, corresponding to the mean value over the set of snapshots or the least-square approximation. The three following values are obtained by applying these approximations to the momentum equation and to the kinetic energy equation (mean value computed from the momentum equation yields irrelevant results):

$$\nu_i = \frac{\langle p_i^{\approx}(A)d_i^{\leq}(A) \rangle}{\langle (d_i^{\leq}(A))^2 \rangle} \text{ (least-square approximation from momentum equation);} \tag{4.5}$$

$$\tilde{\nu}_i = \frac{\langle a_i p_i^{\approx}(A) \rangle}{\langle a_i d_i^{\leq}(A) \rangle} \text{ (mean value from kinetic energy equation);} \tag{4.6}$$

$$\tilde{\nu}_i = \frac{\langle a_i^2 p_i^{\approx}(A)d_i^{\leq}(A) \rangle}{\langle (a_i d_i^{\leq}(A))^2 \rangle} \text{ (least-square approximation from kinetic energy equation).} \tag{4.7}$$

Usual subgrid-viscosity models for LES are based on the budget equation for the resolved kinetic energy, and thus are similar to closures defined by (4.6) and (4.7). Results obtained for several cutoff values are presented in figure 6. Only modes $1 \leq i \leq 87$ are used to compute the eddy viscosity, the other modes being unimportant. The locality of the transfers observed in the preceding section also indicates that most transfers occur within this part of the POD spectrum for the cutoff values considered here.

It is observed that the three definitions yield similar eddy-viscosity profiles which share several properties with the theoretical eddy viscosity in Fourier space for a Kolmogorov spectrum and a sharp-cutoff filter: (i) a cusp is observed near the cutoff as i tends to l (zero viscosity is recovered for $i = l$, since modes higher than 87 are discarded), (ii) $\nu(i|l)$ is a decreasing function of l for fixed i and (iii) the maximum value of the cusp is a nearly constant function of the cutoff index l . These three observations are consistent with the previous statement that the global interactions

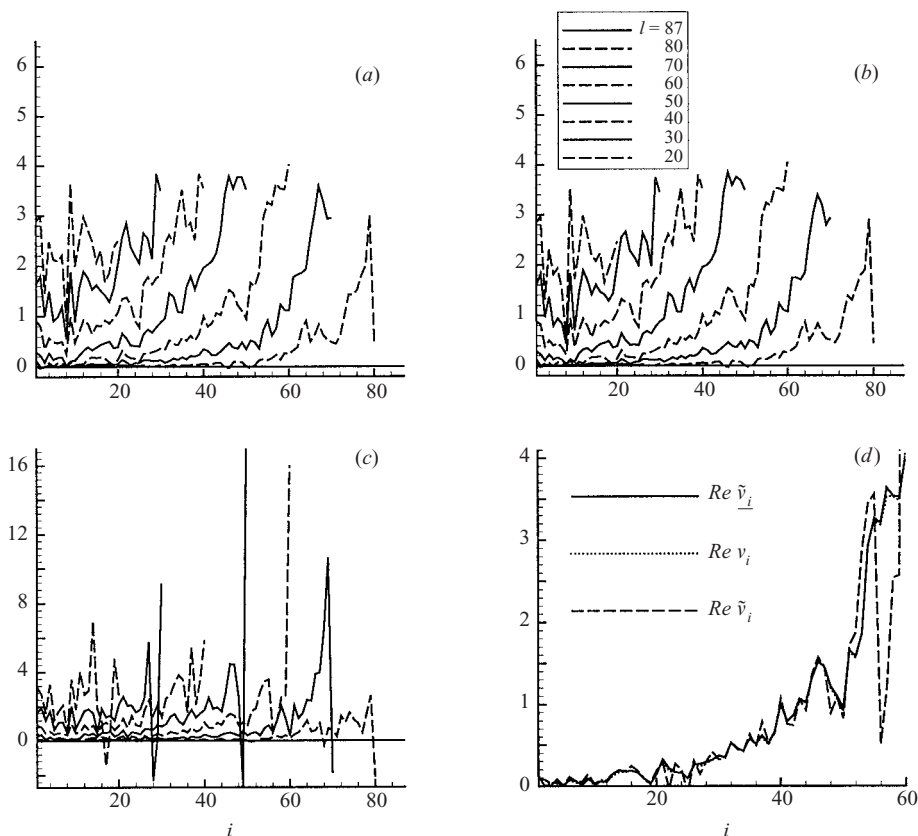


FIGURE 6. Artificial viscosities computed with different cutoff index ($l=87, 80, 70, 60, 40, 30$ and 20): (a) $Re \tilde{v}_i$, (b) $Re v_i$ and (c) $Re \tilde{v}_i$. (d) Comparison of $Re \tilde{v}_i$, $Re v_i$ and $Re \tilde{v}_i$ for $l=60$ (the scale was chosen with respect to the maximum value of $Re \tilde{v}_i$).

between POD modes of increasing index number (i.e. of decreasing energy) are similar to interactions between Fourier modes of increasing wavenumber. The recovery of a cusp-like behaviour near the cutoff on the POD basis is very interesting, since it implies that consistent eddy-viscosity-type models should be mode-dependent. Note that the existence of this cusp is not a straightforward extension of classical Fourier-space results, since the latter disappear for realistic spectrum shapes or smooth filters (Leslie & Quarini 1979).

5. Conclusion

Energy transfers between POD modes representing a turbulent incompressible flow over a backward-facing step have been studied. Using 1000 instantaneous three-dimensional snapshots, the interaction terms have been reconstructed using the Navier–Stokes equations and a Galerkin approach. Energy transfers among POD modes are found to share several properties with their counterparts in Fourier space: (i) they are local in the POD basis in the sense that the transfer term $\Pi(i|j)$ is a rapidly decreasing function of $|i-j|$, (ii) a net forward energy cascade exists, i.e. mode i drains kinetic energy from modes $j < i$ and redistributes it to modes $j > i$ and (iii) a backward energy cascade was observed, since the sign of $\Pi(i|j)$ is not constant

over the 1000 snapshots. These similarities could be explained by POD modes being ranked in decreasing kinetic energy order, and thus associated with smaller and smaller vortical structures. As a consequence, the integrated interactions over the whole computational domain exhibit the same properties as the model interactions within Fourier modes, despite the non-homogeneous character of the present flow.

An interesting consequence is that an eddy-viscosity parameterization of transfers between resolved and unresolved modes in a truncated POD basis shares many properties with its counterpart in Fourier space including the existence of a cusp near the cutoff. Present results suggest that the pseudo-eddy-viscosity $\nu(i|l)$ should explicitly depend on both i and l . Future works will deal with the development of closed truncated POD–Galerkin models.

REFERENCES

- AUBRY, N., HOLMES, P., LUMLEY, J. & STONE, E. 1988 The dynamics of coherent structures in the wall region of a turbulent boundary layer. *J. Fluid Mech.* **192**, 115–173.
- BERKOOZ, G., GUCKENHEIMER, J., HOLMES, P., LUMLEY, J., MARSDEN, J., AUBRY, N. & STONE, E. 1990 Dynamical-systems-theory approach to the wall region. In *AIAA 21st Fluid Dynamics, Plasma Dynamics and Laser Conference*.
- CHOLLET, J. & LESIEUR, M. 1981 Parametrization of small scales of three-dimensional isotropic turbulence utilizing spectral closures. *J. Atmos. Sci.* **38**, 2747–2757.
- DOMARADZKI, J., METCALFE, R., ROGALLO, R. & RILEY, J. 1993 An analysis of subgrid-scale interactions in numerically simulated isotropic turbulence. *Phys. Fluids A* **5**, 1747.
- FOIAS, C., MANLEY, O. & SIROVICH, L. 1990 Empirical and stokes eigenfunctions and the far-dissipative turbulent spectrum. *Phys. Fluids A* **2**, 464–467.
- HOLMES, P., LUMLEY, J. & BERKOOZ, G. 1996 *Turbulence, Coherent Structures, Dynamical Systems and Symmetry*. Cambridge University Press.
- HUNT, J., WRAY, A. & MOIN, P. 1988 Eddies, stream, and convergence zones in turbulent flows. In *Proc. 1988 Summer Program*, pp. 193–208. CTR, Stanford University.
- KRAICHNAN, R. 1971 Inertial-range transfer in two- and three-dimensional turbulence. *J. Fluid Mech.* **47**, 525–535.
- KRAICHNAN, R. 1976 Eddy viscosity in two and three dimensions. *J. Atmos. Sci.* **33**, 1521–1536.
- LABBÉ, O., SAGAUT, P. & MONTREUIL, E. 2002 Large-eddy simulation of heat transfert over a backward-facing step. *J. Numer. Heat Transfer A* **42**, 73–90.
- LESLIE, D. & QUARINI, G. 1979 The application of turbulence theory to the formulation of subgrid modelling procedures. *J. Fluid Mech.* **91**, 65–91.
- PODVIN, B. 2001 On the adequacy of the ten-dimensional model for the wall layer. *Phys. Fluids* **13**, 210–224.
- PODVIN, B. & LUMLEY, J. 1998 A low-dimensional approach for the minimal flow unit. *J. Fluid Mech.* **362**, 121–155.
- REMPFER, D. & FASEL, H. 1994 Dynamics of three-dimensional coherent structures in a flat-plate boundary layer. *J. Fluid Mech.* **275**, 257–283.
- SAGAUT, P. 2002 *Large Eddy Simulations for Incompressible Flows*, 2nd Edn. B. Springer.
- UKEILEY, L., CORDIER, L., MANCEAU, R., DELVILLE, J., GLAUSER, M. & BONNET, J. 2001 Examination of large-scale structures in a turbulent plane mixing layer. Part 2. Dynamical systems model. *J. Fluid Mech.* **441**, 67–108.
- WEBBER, G., HANDLER, R. & SIROVICH, L. 1997 The Karhunen–Loève decomposition of minimal channel flow. *Phys. Fluids* **9**, 1054–1066.
- WEBBER, G., HANDLER, R. & SIROVICH, L. 2002 Energy dynamics in a turbulent channel flow using the Karhunen–Loève approach. *Intl J. Numer. Meth. Fluids* **40**, 1381–1400.
- YEUNG, P., BRASSEUR, J. & WANG, Q. 1995 Dynamics of direct large-small scale couplings in coherently forced turbulence: concurrent physical and Fourier-space views. *J. Fluid Mech.* **283**, 43–95.
- ZHOU, Y. & VAHALA, G. 1993 Reformulation of recursive-renormalization-group based subgrid modeling of turbulence. *Phys. Rev. E* **47**, 2053.